

SOA-based all-optical switch with subpicosecond full recovery

H. Ju, S. Zhang, D. Lenstra*, H. de Waardt, E. Tangdiongga, G. D. Khoe
and H. J.S. Dorren

COBRA Research Institute, Eindhoven University of Technology,
P.O. Box 513, 5600 MB, Eindhoven, The Netherlands.

*Also with the Division of Physics and Astronomy FEW, Vrije Universiteit,
Amsterdam, The Netherlands
h.ju@tue.nl

Abstract: We investigate all-optical switching in a multi-quantum-well semiconductor optical amplifier-based nonlinear polarization switch using optical pulses with duration of 200 fs at a central wavelength of 1520 nm. We show full recovery of the switch within 600 fs, in both the gain and absorption regime. We discuss the switching and recovery mechanisms using numerical simulations that are in qualitatively good agreement with our experimental data.

©2005 Optical Society of America

OCIS codes: (250 5980) semiconductor optical amplifier; (320, 7110) ultrafast nonlinear optics

References and links

1. T. Durhuus, B. Mikkelsen, C. Joergensen, S. L. Danielsen and K. E. Stubkjaer, "All-Optical Wavelength Conversion by Semiconductor Optical Amplifiers," *J. Lightwave Technol.* **14**, 942-954 (1996).
2. D. Nasset, T. Kelly and D. Marcenac, "All-optical wavelength using SOA nonlinearities," *IEEE Communications Magazine* **36**, 56-61 (1998).
3. K. L. Hall, et al., "Nonlinearities in active media," In *Nonlinear Optics In Semiconductors II. Semiconductors and Semimetals*, **59**, E. Garmire and A. Kost, (Academic Press, San Diego, 1999).
4. N. S. Patel, K. L. Hall, K. A. Rauschenbach, "40Gbit/sec cascaded all-optical logic with an ultrafast nonlinear interferometer," *Opt. Lett.* **21**, 1466-14688 (1996).
5. A. D. Ellis, A. E. Kelly, D. Nasset, D. Pitcher, D. G. Moodie, and R. Kashyap, "Error free 100 Gbit/s wavelength conversion using grating assisted cross-gain modulation in 2mm long semiconductor amplifier," *Electron. Lett.* **34**, 1958-1959 (1998).
6. M. F. C. Stephens, M. Asghari, R.V. Penty, and I. H. White, "Demonstration of ultrafast all-optical wavelength conversion utilizing birefringence in semiconductor optical amplifiers," *IEEE Photon. Technol. Lett.* **9**, 449-451 (1997).
7. H. Soto, D. Erasme, and G. Guekos, "Cross-polarization modulation in semiconductor optical amplifiers," *IEEE Photon. Technol. Lett.* **11**, 970-972 (1999).
8. D. Cotter, R. J. Manning, K. J. Blow, A. D. Ellis, A. E. Kelly, D. Nasset, I.D. Phillips, A. J. Poustie, and D. C. Rogers, "Nonlinear optics for high-speed digital information processing," *Science* **286**, 1523 (1999).
9. G. Lenz, E. P. Ippen, J. M. Wiesenfeld, M. A. Newkirk, and U. Koren, "Femtosecond dynamics of nonlinear anisotropy in polarization insensitive semiconductor optical amplifiers," *Appl. Phys. Lett.* **68**, 2933 (1996).
10. S. Nakamura, Y. Ueno, and K. Tajima, "Ultrafast (200-fs switching, 1.5-Tb/s demultiplexing) and high-repetition (10 GHz) operations of a polarization discriminating symmetric Mach-Zehnder all-optical switch," *IEEE Photon. Technol. Lett.* **10**, 1575 (1998).
11. H. Ju, S. Zhang, H. de Waardt, G.D. Khoe and H.J.S. Dorren, "Ultrafast all-optical switching by pulse-induced birefringence in a multi-quantum-well semiconductor optical amplifier," in *Technical Digest CLEO (San Francisco, 2004)*, CFJ1.
12. X. Yang, D. Lenstra, G. D. Khoe, H. J. S. Dorren, "Nonlinear polarization rotation induced by ultrashort optical pulses in a semiconductor optical amplifier," *Opt. Commun.* **223**, 169 (2003).
13. A.K. Mishra, X. Yang, D. Lenstra, G.D. Khoe and H.J.S. Dorren, "Wavelength conversion employing 120 fs optical pulses in an SOA-based nonlinear polarization switch," *IEEE J. Sel. Quantum Electron.* (to be published).

14. H. J. S. Dorren, D. Lenstra, Y. Liu, M. T. Hill, and G. D. Khoe, "Nonlinear polarization rotation in semiconductor optical amplifiers: theory and application to all-optical flip-flop memories," *IEEE J. Quantum Electron.* **39**, 141-147 (2003).
-

1. Introduction

All-optical switches based on nonlinearities in Semiconductor Optical Amplifiers (SOAs) are considered important building blocks in optical telecommunication systems [1-4]. Several SOA-based switching techniques have been demonstrated. Optical switches utilizing four-wave-mixing in an SOA are independent of the modulation format but they have low conversion efficiency and also the input light needs to be polarization-matched [2]. Optical switches based on cross-gain modulation (XGM) in a single SOA have been demonstrated at 100 Gbit/s, but this approach leads to a degradation of the extinction ratio [5]. Interferometric optical switches based on cross-phase modulation in combination with XGM in SOAs lead to an improved extinction ratio and can also be used to realize inverted and non-inverted conversion. Furthermore, this concept can be utilized for signal reshaping [1,2].

In this letter, we focus on optical switches based on nonlinear polarization rotation in a single SOA [6,7] and present new results that clearly show the potential of this concept for switching at ultrahigh repetition rates. Essential for SOA-based all-optical switches operating at ultrahigh repetition rates is absence of a carrier lifetime-imposed-long-lived tail, which prevents pattern effects on the switched data-stream from occurring [8]. Switching of ultrashort optical pulses in an SOA-based nonlinear polarization switch has been investigated in [9] in the context of a fundamental investigation of nonlinear anisotropy in polarization-independent SOAs. The results in [9] suggest that ultrafast operation in an SOA-based nonlinear polarization switch is not possible due to a long-lived tail in the switch recovery.

In this paper, we present two important new results. Firstly, we show that it is possible to obtain full recovery of an SOA-based nonlinear polarization switch on a sub-picosecond timescale. We find, in both the gain and absorption regime that the nonlinear polarization switch can fully recover within 600 fs for properly chosen pulse energies. This implies that the nonlinear polarization switch should be able to realize a speed comparable to the results presented in [10]. Our second important result is that the nonlinear polarization switch can be operated with control pulses that contain 49 fJ of energy, which is a few orders lower than the results presented in [10]. This opens the door to optical switching in a single SOA at repetition rates greater than 640 Gbit/s.

2. Experimental set-up

A schematic of our experimental set-up is shown in Fig. 1. An optical parametric oscillator (OPO) pumped by a Ti:Sapphire laser is used to generate optical pulses with duration of 200 fs at a central wavelength of ~ 1520 nm. The pulses output the OPO with a repetition rate of 76 MHz. A polarizing beam splitter (PBS) is used to split the linearly polarized OPO output into two beams, i.e. a pump beam (s-polarization) and a probe beam (p-polarization). The polarizations of the pump and probe beams are controlled, by adjusting the angle of quarter-wave plates QP1 and QP2, leading to a p-polarized pump beam and a s-polarized probe beam between the PBS and the half-wave plate (HP). The pump and probe light is focused into the SOA by using a microscope objective lens with a focal length of 4.6 mm (Numerical aperture = 0.65) while being collimated out of the SOA by another microscope objective lens with a numerical aperture of 0.45. Our nonlinear waveguide is a multi-quantum-well InGaAsP/InGaAs SOA with a length of 250 μm . The SOA has 15 layers that consist of compressive-strained InGaAsP quantum wells and tensile-strained InGaAs barriers. The optical bandwidth is 34 nm and the peak of the SOA gain spectrum occurs at ~ 1525 nm for an injection current of 100 mA. The polarization dependence of the SOA gain is about 5 dB (for small signal cw light). The SOA is operated using injection currents (I) in a range between 0 mA to 200 mA.

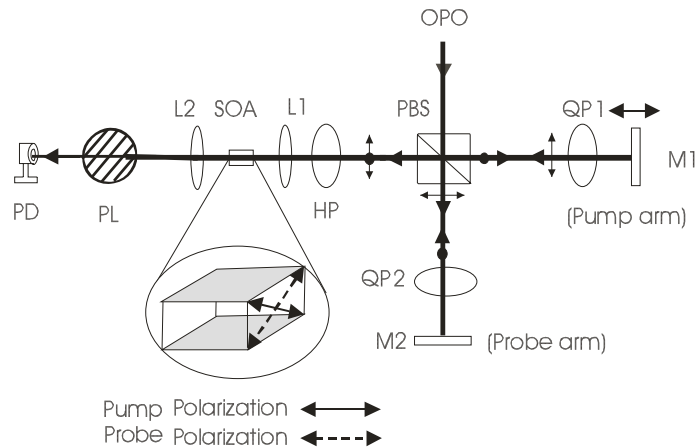


Fig. 1. A schematic of the experimental setup. OPO: Optical parametric oscillator, PBS: Polarizing beam splitter, QP1-2: Quarter-wave plates, M1-2: Mirrors, HP: Half-wave plate, L1-2: Microscope objective lenses, SOA: Semiconductor optical amplifier, PL: Polarizer, PD: Photodetector.

A polarizer (PL) is used to minimize the pump transmission at the SOA output. This experimental set-up allows measurements of the pump-induced birefringence, by measuring the reduction of the transmission of the probe light through the polarizer PL as a function of pump-probe time delay. The pump-probe delay is controlled by changing the position of mirror M1, which was mounted on a delay stage. The half-wave plate HP is used to control the orientations of the polarizations of the pump and probe beams with respect to the SOA layers, while maintaining the mutual orthogonality between the pump and probe pulses. Unwanted pump-probe interference effects due to polarization conversion in the waveguide and pump-leakage through the polarizer PL cause noise in the detection system, which is filtered out by an electronic low-pass filter. The minimum detectable pulse energy in the detection system at the SOA output is ~ 0.08 fJ.

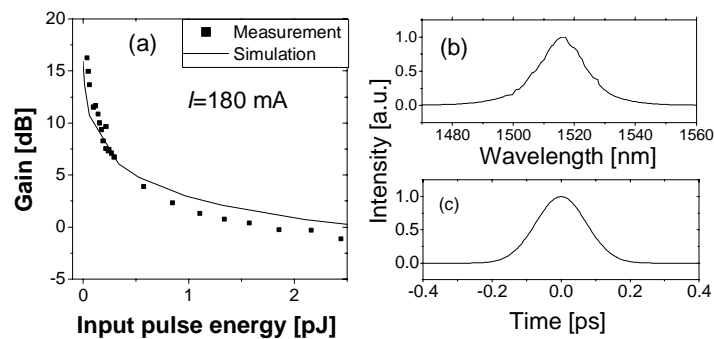


Fig. 2. (a) The SOA gain as a function of an input-pulse energy for input polarization of 45 degrees with respect to the SOA layers. (b) : Measured input pulse spectrum, (c) : Input pulse intensity estimated from (b).

The set-up shown in Fig. 1 acts as a nonlinear polarization switch as follows. In the calibration process, the probe pulse propagates ahead of the pump pulse by more than one picosecond, while the angle of the polarizer PL is set such that the pump light is maximally blocked. If the pump and probe pulses overlap, the pump-induced nonlinear birefringence causes the polarization of the probe pulse to change, so that its transmission through PL is reduced.

3. Results and discussion

The gain saturation of the SOA is shown in Fig. 2(a) in case of an injection current of 180 mA. The input polarization of the optical pulses was 45 degrees with respect to the SOA layers. The gain saturation increases with the input-pulse energy. Figure 2(b) shows the measured spectrum of OPO pulses while Fig. 2(c) represents the Gaussian temporal shape of pulse intensity, which is estimated from (b) indicating that the pulse duration is approximately 180 fs.

We investigate switching in the configuration of Fig. 1 by measuring the probe transmission as a function of the pump-probe delay time. Figure 2 shows typical measurements of normalized probe transmission through PL as a function of the pump-probe time-delay. The angle of HP is set such that the mutually orthogonal linear polarizations of pump and probe were oriented under 45 degrees with respect to the SOA layers at the SOA input, as shown in Fig. 1.

Figure 3(a) shows the trace in case of zero injection current, while in Fig. 3(b) the SOA injection current was 200 mA and in Fig. 3(c) 180 mA. For the case of zero injection current, the input pump and probe pulse energies are 3.1 pJ and 0.34 pJ respectively. It follows from Fig. 3(a) that the maximum reduction of the probe transmission is about 30 % and that the transmission fully recovers within 525 fs. This full recovery is reproduced with pump pulse energies in a range of 1.7 pJ to 3.7 pJ. For the case that the amplifier is pumped with 200 mA of current, the input pump and probe pulse energies are 49 fJ and 5.3 fJ, respectively. The small-signal gain is approximately 16 dB. Figure 3(b) shows that the maximum reduction of the probe transmission is approximately 70% and that the transmission fully recovers in 570 fs. This full recovery is reproduced for 160 mA and 200 mA with respective pump pulse energies of 49 fJ and 58 fJ.

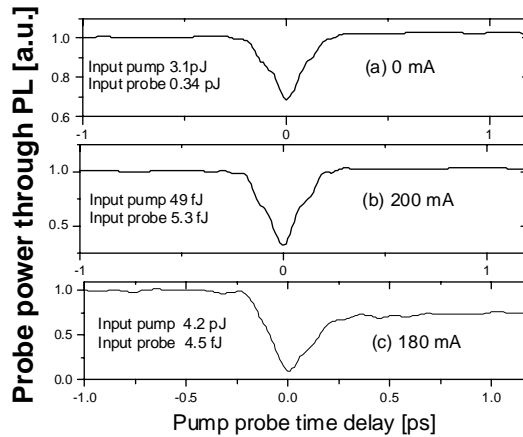


Fig. 3. The normalized probe transmissions through PL at injection currents of 0 mA (a), 200 mA (b) and 180 mA (c) respectively.

Note that in both Figs. 3(a) and 3(b), no long-lived tail is visible in the probe transmission. However, we have observed a long-lived tail in the recovery of the switch for injection current higher than 60 mA and pump pulse energies larger than 1 pJ [11]. This is illustrated in Fig. 3(c) in which the SOA is pumped with 180 mA, while the input pump and probe pulse energies are 4.2 pJ and 4.5 fJ respectively. Figure 3(c) shows a maximum reduction of the probe transmission of 90 %, but also shows a long-lived tail in the SOA recovery.

Figure 4 shows a simulation of the switching experiment. The model for pulse propagation through the SOA is in the fashion of [12,13] and the model for the nonlinear polarization switch can be found in [14]. The probe transmission through PL, $P(\tau)$ is given by:

$$P(\tau) \sim \int_{-T/2}^{T/2} \{2[P^{TE}(t,\tau)P^{TM}(t,\tau)]^{1/2} \cos[\Delta\phi_{NL}(t,\tau)] + P^{TE}(t,\tau) + P^{TM}(t,\tau)\} dt \quad (1)$$

where $P^{TE(TM)}(t,\tau)$ is the probe power for the TE (TM) component and in $\Delta\phi_{NL}(t,\tau)$ is the difference between the pump-induced phase shift in the TE mode and that in TM mode of the probe light:

$$\Delta\phi_{NL}(t,\tau) = \frac{1}{2}\alpha \int_0^L [\Gamma^{TE} g^{TE}(z,t,\tau) - \Gamma^{TM} g^{TM}(z,t,\tau)] dz. \quad (2)$$

Here, α is the line-width enhancement factor, $g^{TE(TM)}(z,t,\tau)$ represents the SOA gain function and $\Gamma^{TE(TM)}$ is the confinement factor for the $TE(TM)$ mode. As shown in [12, 13], the gain functions $g^{TE(TM)}(z,t,\tau)$ account for ultrafast carrier dynamics driven by spectral hole-burning (SHB), two-photon absorption (TPA) and free-carrier absorption (FCA). The parameters used in the modeling are given in table 1 including the time constants for electron-electron scattering (τ_{ee}), hole-hole scattering (τ_{hh}), carrier-phonon scattering (τ_{LO}) and carrier-life-time (τ_L) that determine the time-response of the device. As discussed in [12, 13], the direct effect due to TPA in $\Delta\phi_{NL}(t,\tau)$ has cancelled out. Note that $P^{TE(TM)}(t,\tau)$, $\Delta\phi_{NL}(t,\tau)$ and $g^{TE(TM)}(z,t,\tau)$ represent the optical power, nonlinear phase-shift and gain as a function of real time t , pump-probe time-delay τ and position z in the SOA, respectively. Averaging over the detector response time T makes that the observed photo-current only depends on τ .

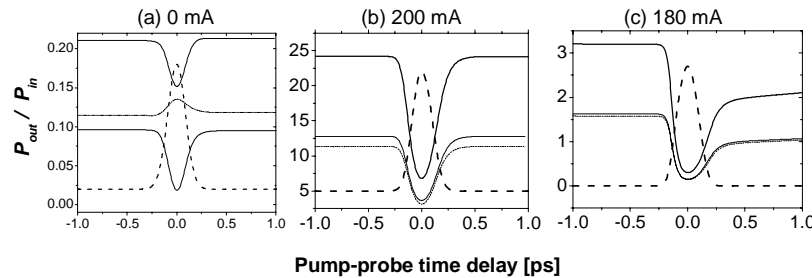


Fig. 4. A numerical simulation of probe transmission $P(\tau)$. $P(\tau)$ is normalized to the input probe power. The bold solid curves are the probe transmissions through the polarizer PL, the thin solid curves represent the contribution due to nonlinear birefringence, the thin dashed curves represent the amplitude change by the gain saturation, and the bold dashed lines are the output pulse intensity of pump light.

Our modeling indicates that the shape of $P(\tau)$ is determined by the interplay of two effects. The first effect is the pump-induced birefringence represented by the first term of the integrand of Eq. (1) and always leads to a decrease of the probe transmission through PL. The second effect is the pump-induced change of probe amplitude (gain saturation), which is represented by the second and third terms of the integrand of Eq. (1), and leads to an increase of the probe transmission in the absorption regime, but to a decrease in the gain regime. These two effects are illustrated in Fig. 4 where the bold solid curves represent the probe transmissions through PL while the thin solid curves represent the first effect and the thin dashed curves represent the second effect as mentioned above. The values on the vertical axes in Fig. 4 are normalized with respect to the input probe powers. The bold solid curve is the

sum of the other two curves. In all three cases, the nonlinear birefringence always leads to a decrease of the probe transmission. Conversely, the nonlinear gain saturation leads to an increase of the probe transmission through PL for the case of 0 mA injection current (due to stimulated absorption) but to a decrease of the probe transmission through PL for the cases of an injection current of 200 mA and 180 mA (due to stimulated emission).

For $I=0$ mA, the effects of the recovery of the gain saturation (thin dashed curve) and the recovery of the nonlinear birefringence (thin solid curve) cancel each other out, so that no long-lived tail is visible in the recovery of the probe transmission. For $I = 200$ mA, the recovery of both the birefringence and the gain shows no long-lived tail, due to the low pulse energies. The gain recovery effects via carrier-phonon scattering on a timescale of 1 ps is small, due to the little FCA and stimulated emission. Finally, if the pump-pulse energy is increased, a long-lived tail appears in the recovery of the gain and birefringence. Note that the (nonlinear) cosine operation in the first term of Eq. (1) suppresses the effect of a small long-lived tail in the birefringence and imposes a narrowing effect on the probe pulse transmission.

Table 1. Parameters used in the simulation results

Parameter	Value	Parameter	Value
α for $I=180, 200\text{mA}$	2	τ_{ee}	70 fs
α for $I=0$ mA	8.5	τ_{hh}	30 fs
$\Gamma^{TE/TM}$	0.23/0.15	τ_{LO}	700 fs
τ_p (input pulse length)	180 fs	τ_L	200 ps

4. Conclusions

We have investigated sub-picosecond optical switching in an SOA based nonlinear polarization switch. We have shown that the nonlinear polarization switch can fully recover within 600 fs if the control pulse energy is sufficiently low. We observed a maximum reduction of the probe transmission of 30% for zero injection current and a maximum reduction of 70% for an injection current of 200 mA. Numerical analysis of the switching process reveals that two effects contribute to the switch output: nonlinear phase changes (birefringence) and amplitude changes by gain saturation. For zero injection current, these processes oppose each other, which makes that the long-lived tail cancels out at the output of the switch. We have also pointed out that it is possible to suppress a long-lived tail in the gain regime by using pump pulses with sufficiently low energies. In this regime, the ultrafast full recovery of the switch suggests that at high repetition rates, the switched data will not be contaminated with pattern-effects, so that error-free operation is feasible.

An optical switch that fully recovers on subpicosecond timescales that also consumes low power is interesting for use in telecommunication systems. In particular, such switches could play a role as demultiplexers in OTDM systems operated at ultra-high data-rates or in wavelength converters. The 49 fJ control pulses at a repetition-rate of 640 Gbit/s gives an average power of 31 mW. This is sufficiently low to be handled by the SOA. Preliminary experimental results employing pulses with duration of 300 fs at a repetition rate of 160 Gbit/sec confirm that error-free optical switching using control pulses at these low power-levels is feasible.

Acknowledgments

This work was supported by the Netherlands Organization for Scientific Research (NWO), the Technology Foundation STW and the Ministry of Economic Affairs through respectively the NRC Photonics grant, the Innovational Research Incentives Scheme program.